

Novel Source of Nonlocality in the Optical Model

M. I. Jaghoub^{1*}, M. F. Hassan¹, G. H. Rawitscher²

¹ Department of Physics, University of Jordan, P. C. 11942, Amman, Jordan

² Department of Physics, University of Connecticut, Storrs, CT 06269, USA

November 19, 2018

Abstract

In this work we fit *neutron* - ^{12}C elastic scattering angular distributions in the energy range 12 to 20 MeV, by adding a velocity dependent term to the optical potential. This term introduces a wave function gradient, whose coefficient is real and position dependent, and which represents a nonlocality. We pay special attention to the prominent backscattering minima which depend sensitively on the incident energies, and which are a tell-tale of nonlocalities. Reasonable fits to the analyzing power data are also obtained as a by-product. All our potentials have the form of conventional Woods - Saxon shapes or their derivatives. The number of our parameters (12) is smaller than the number for other local optical potentials, and they vary monotonically with energy, while the strengths of the real and imaginary parts of the central potential are nearly constants. Our nonlocality is in contrast to other forms of nonlocalities introduced previously.

PACS numbers: 24.10.Ht, 25.40.Dn, 24.70.+s

*E-mail address: mjaghoub@ju.edu.jo

1 Introduction

Since its inception in 1954 [1] the nuclear optical model has undergone many improvements and refinements. Two main theoretical approaches emerged. One, the microscopic non relativistic approach, that consists in folding a two-body nucleon-nucleon g -matrix into the nucleon distributions contained in the target nucleus [2], and iteratively includes the many-body aspects of the nucleus [3]. The other approach makes use of the Dirac equation to describe the wave function of the incident nucleon, and is of a more phenomenological nature [4]. Both approaches provide almost equally good descriptions of the nucleon scattering cross sections and polarizations in a range of energies, as demonstrated recently for a representative number of target nuclei [5]. The Dirac approach automatically introduces a nonlocality through the Darwin term, but does not allow for the Pauli exclusion principle, while the non relativistic approach does include the latter [5]. It is also found that the Dirac approach requires a much smaller energy dependence of the Dirac optical potentials than the corresponding non relativistic potentials, which suggests that this difference is related to the nonlocality present in the Dirac procedure [6, 7].

There should be at least two sources of nonlocality in the conventional, non relativistic optical model: The first is due to the Pauli exclusion principle. This nonlocality is usually taken into account by writing the overall wave function as a Hartree-Fock determinant, and it leads to an additional integral term in the Schrödinger equation. Other methods also exist [8]. The second is a "Feshbach nonlocality", that is due to the coupling of the inelastic excitations to the ground state in the elastic channel during the scattering process. Since the form of this nonlocality is difficult to quantify, it usually is ignored, or taken into account by numerically coupling a few inelastic channels to the elastic channel [9]. Another method, proposed by Perey and Buck [10], is to assume an "ad hoc" nonlocality expression in terms of a combination of exponential functions of position, and obtain the local equivalent potential in the Schrödinger equation. The Perey-Buck nonlocality is found to provide an energy dependence of the central local equivalent optical potential that is in agreement with the phenomenological energy dependence, and leads to Perey Damping factors that are roughly similar to the ones in the Dirac optical model approach [7]. Other forms of nonlocalities have also been explored, notable among them being a parity dependent term in the optical model [11, 12], which led to a tentative justification in terms of the Feshbach

channel coupling effect [13, 14]. In a recent work, a nonlocal optical potential which has the Perey-Buck type spatial dependence was employed in the calculations of three-body direct nuclear reactions. An important nonlocality effect has been found for some transfer reactions [15].

It is important to understand the presence of nonlocalities, because the corresponding local representation of the optical model leads to a phase equivalent wave function that is larger in magnitude than the corresponding nonlocal wave function (the Perey damping factor), and hence leads to discrepancies in the distorted wave approximation calculations (DWBA) of inelastic or rearrangement processes, which in turn lead to errors in obtaining the shell-model occupation numbers of the target nucleus.

The purpose of this paper is to introduce yet another nonlocality term into the optical potential, that is expressed by the presence of a derivative term in the Schrödinger equation. The coefficient is a position-dependent effective mass of the nucleon embedded in the nuclear medium, resulting from the interaction with the other nucleons. The concept of an effective mass is relevant to the nuclear many body problem in connection with the energy-density functional approach. Here, the nonlocal terms are usually interpreted as a three-dimensional position-dependent effective mass [16]. By considering the most general kinetic energy operator for a particle with a spatially variable mass [17], the Schrödinger equation can be recast in a form that describes a constant mass moving in a velocity-dependent potential [18]. Our preliminary justifications for this nonlocality is based on the excellent fits to low-energy $N-^{12}C$ elastic scattering data which we achieve. In particular, the fits reproduce very well the pronounced minima corresponding to large angle backward scattering, which are usually associated with nonlocalities [4]. Even though we did not include the analyzing power in the search for parameters in the fit to the elastic cross sections, we also obtained reasonably good fits to the experimental analyzing powers, a result that supports the presence of our velocity dependent term. It must be stressed, however, that our velocity dependent term is not similar [19] to the velocity dependent Darwin term that occurs in the Dirac based formulation [20], because the Darwin term is complex, while our effective mass is real. Further, the Darwin term is closely coupled to the spin orbit potential in the Dirac formulation, while our spin orbit term is completely independent of the velocity term [19]. In a future investigation [19] we will study the physical origin of our nonlocality, in particular, whether it approximately simulates the effect of channel coupling to excited states, or whether it simulates exchange effects,

or introduces a new type of nonlocality.

Velocity-dependent potentials have long been used in nuclear and atomic physics. For example, such a potential was introduced to explain the predominantly p -wave nature of the pion-nucleon scattering [21]. In addition, a model assuming a velocity-dependent nucleon-nucleon interaction reproduced the 1S , 1D and 1G singlet-even phase shifts required for the description of nucleon-nucleon scattering cross sections [22]. In the field of atomic physics the scattering of electrons from atomic oxygen and neon was studied in the frame work of an analytic velocity-dependent potential [23]. In addition, the effective mass formulation has been introduced into condensed matter physics to describe the dynamics of electrons in semiconductor hetrostructures such as compositionally graded crystals [24] and quantum dots [25]. Further, scattering of electrons on disordered double-barrier hetrostructures has been considered in Ref. [26]. Finally, one of us presented perturbation formalisms that accounts for the effect of a small perturbing velocity-dependent potential on the bound-state energies and the scattering phase shifts. [27, 28].

2 The velocity-dependent term

In this section we shall briefly outline the effective mass formalism that leads to a velocity-dependent term. As mentioned above, the most general kinetic energy term used to describe a spatially variable mass $m(r)$ is given as [17]

$$T = -\frac{\hbar^2}{2m} \left[m^\delta(r) \nabla m^\beta(r) \nabla m^\gamma(r) + m^\gamma(r) \nabla m^\beta(r) \nabla m^\delta(r) \right]. \quad (1)$$

Since the mass depends on position it no longer commutes with the momentum operator and the ambiguity parameters obey the constraint $\delta + \beta + \gamma = -1$ [17]. Interesting works were carried out to determine a unique set of ambiguity parameters. For example, by considering the one-dimensional Schrödinger equation for a spatially variable mass $m(x)$ it was suggested that there is a privileged ordering, namely, $\delta = 0, \beta = -1$ which was obtained by demanding $[m(x)]^{-1} \partial/\partial x$ be continuous at the point of discontinuity of $m(x)$ [29]. For this set of parameters, the potential functions for the one- and three-dimensional Schrödinger equations were obtained in addition to explicit expressions for the bound state energy spectrum and the corresponding wave functions [30]. In addition, the formalism of supersymmetric

quantum mechanics is extended to the one-dimensional Schrödinger equation with a spatially variable mass [31].

Using the above form of T and choosing the same set of parameters ($\delta = 0, \beta = -1$) the corresponding radial Schrödinger equation reads:

$$-\frac{\hbar^2}{2m} \left\{ \frac{d^2}{dr^2} - \frac{m'}{m} \left[\frac{d}{dr} - \frac{1}{r} \right] - \frac{l(l+1)}{r^2} \right\} v(k, r) = [E - V(r)] v(k, r), \quad (2)$$

where $m \equiv m(r)$ and $v(k, r) = rR(r)$ is the reduced wave function and the prime denotes a derivative with respect to r . By making the substitution

$$\frac{1}{m} = \frac{1 - \rho(r)}{m_0}, \quad (3)$$

where $\rho(r)$ is some isotropic function of the radial variable r and m_0 is a constant mass, equation (2) reduces to

$$(1 - \rho)v''(r) - \left[v'(r) - \frac{v(r)}{r} \right] \rho' - (1 - \rho) \frac{l(l+1)}{r^2} v(r) = \frac{2m_0}{\hbar^2} [V(r) - E] v(r), \quad (4)$$

where the dependencies of the reduced wave function on k and $\rho(r)$ on r have been suppressed for clarity of presentation. This is exactly the same equation one obtains when starting from the usual Schrödinger equation but with a velocity-dependent potential of the form:

$$\begin{aligned} \hat{V}(r, p) &= V(r) + \frac{\hbar^2}{2m_0} \nabla \cdot \rho(r) \nabla \\ &= V(r) + \frac{\hbar^2}{2m_0} \left[\rho(r) \nabla^2 + \nabla \rho(r) \cdot \nabla \right] \end{aligned} \quad (5)$$

The second term on the right hand side results in a kinetic energy term that combines with the corresponding term in the Schrödinger equation. The third term, however, is proportional to the gradient of $\rho(r)$ in addition to the gradient of the wave function. Once more, it is worth mentioning that the gradient terms are not identical to those obtained when the Dirac formalism is extended to the non relativistic regime.

3 Velocity-dependent optical potential

One of the nonlocalities that we propose to be present in the optical model is due to the change in mass of the nucleon arising from its interactions with

other nucleons inside the nucleus. Our aim in this work is to determine to what extent the inclusion of an "ad hoc" velocity-dependent term can simulate such a nonlocality. For this purpose we shall introduce a gradient part resulting in a velocity-dependent optical potential of the form given in equation (5) with the conventional optical model part given by,

$$V(r) = -V_0 f(r, x_0) + 4ia_w W \frac{df(r, x_w)}{dr} + 20 \left(\frac{\hbar}{\mu c} \right)^2 (V_{so} + iW_{so}) \frac{1}{r} \frac{df(r, x_{so})}{dr} \vec{\sigma} \cdot \vec{I}, \quad (6)$$

where μ is a constant neutron-nucleus reduced mass. For the gradient term we define

$$\rho(r) = \rho_0 a_\rho \frac{df(r, x_\rho)}{dr}, \quad (7)$$

where x_0 stands for (r_0, a_0) and so on for the rest of the terms. The function $f(r, r_j, a_j)$ is of a Woods-Saxon form, namely,

$$f(r, r_j, a_j) = \frac{1}{1 + \exp[(r - r_j A^{1/3})/a_j]}, \quad (8)$$

where A is the mass number of the target nucleus. Clearly, $\rho(r)$ is a surface term, which may be interpreted as the gradient of the mass density of the target nucleus [21]. In view of this, one would expect the effect of including this term to be important closer to the nuclear surface rather than deep in the interior of the target nucleus. In fact our best fits are obtained with the peak of $\rho(r)$ close to the nuclear surface.

In an attempt to reduce the number of fit parameters we have used the same geometry parameters for the real and imaginary parts of the spin-orbit term. Our model has 12 fit parameters compared to the conventional optical potentials which have a number of fit parameters ranging from nine to twenty. For example, in a previous work [33], the conventional optical potential with nine fit parameters was used to fit the neutron-nucleus elastic angular distribution data for 1- p shell nuclei ranging from ${}^6\text{Li}$ to ${}^{13}\text{C}$. The bombarding neutron energies fell in the range 7 - 15 MeV, which does not include the pronounced large-angle backward scattering minima at 18 and 20 MeV. Further, as the authors stated, the emphasis was put on reproducing the overall behavior of the angular distributions and not the exact details as the low energy region is endowed with resonances. A more recent work presented new global and local optical potentials for neutrons and protons with incident energies ranging from 1 keV to 200 MeV for nuclei in the mass

range $24 \leq A \leq 209$ [34]. Each of the local optical potentials included 20 fit parameters and resulted in excellent fits to the experimental data. The strength of the central real potential showed the largest variation as a function of the incident energy. Furthermore, energy-dependent global Dirac optical potentials also resulted in excellent fits to proton elastic scattering data corresponding to incident energies in the range 20 - 1040 MeV for a number of light and heavy nuclei. The number of optical potential parameters is about 24 and the data sets were restricted to observables at angles less than 90 degrees so as to avoid the effect of nonlocalities, which were believed to be important at large back scattering angles [4, 14].

4 Velocity-dependent optical potential fits

As mentioned in the introduction there are sources of nonlocalities in the non relativistic optical potential, such as exchange processes, and coupling of the inelastic excitations to the ground state of the elastic channel. In this work we introduce yet another source of nonlocality presumably resulting from the change in mass of the incident nucleon due to its interactions with the other nucleons inside the nucleus, and we ignore the other two. In order to simulate such a "medium" nonlocality, we have added a velocity-dependent term to the optical potential. This introduces a wave function gradient term whose coefficient is real and position dependent. As outlined in section 2, the Schrödinger equation describing a spatially variable mass can be made identical to a Schrödinger equation describing the dynamics of a constant mass moving in a velocity-dependent potential of the form given in equation (5). Our aim is to test the ability of such a velocity-dependent optical potential to simulate the effective mass nonlocality especially in the backward (large angle) scattering region which has long been associated with nonlocalities [4, 14].

Using the proposed velocity dependent optical potential (VDOP) with $V(r)$ and $\rho(r)$ given by equations (6) and (7) respectively, we searched for sets of parameters that fit the $N-^{12}C$ angular distribution elastic scattering data in the low-energy 12–18 MeV range. Lower energies were not considered in order to avoid resonance effects. The source of the data is the Evaluated Nuclear Data File [32]. The data showed pronounced large angle backward scattering minima that are very sensitive to energy changes, thus signifying sources of nonlocalities. We varied the parameters until a best fit to the

elastic angular distributions are obtained. The fits are shown in Figures 1 and 2 and our best fit parameters are presented in Tables 1 and 2. Clearly, the VDOP has reproduced well the experimental data, most notably the pronounced large-angle, backscattering minima at 18 and 20 MeV. The quality of the fits at the large back angle minima is found to be sensitive to both the spin-orbit and to the velocity-dependent terms. Further, the peak of the spin-orbit term monotonically moved into the nuclear interior as the incident energy increased. As shown in Figure 3, at 12 MeV incident energy, the peak of $\rho(r)$ is at the outer edge of the real central potential. However, as the energy increased the peak moved into the nuclear interior but remained within the region of the diffused edge of the central potential. This supports the hypothesis that $\rho(r)$ is related to the gradient of the target's mass density [21]. The strengths of the real and imaginary potentials V_0 and W were nearly stable as a function of incident energy especially for $E \geq 16$ MeV.

For a perfect theory, one would expect the fit parameters to have a smooth variation with energy. By inspecting Tables 1 and 2 it can be seen that our parameters generally vary smoothly with energy. However, some of the parameters at $E = 16$ MeV are quite different from the corresponding ones at neighboring higher and lower energies. This may be due to the fact that there are several energy-dependent additional effects in the nucleon-nucleus elastic scattering process that are still explicitly left out at the present stage. One is the exchange effect, and the other is a channel coupling effect. The latter involves a Feshbach-like polarization potential, that is known to be angular momentum and energy dependent and is nonlocal. In a future work, it is our hope to take such effects into account by re-expressing both effects in terms of gradient terms, thus modifying our proposed velocity-dependent optical potential. This is expected to result in an even smoother variation of our parameters with energy.

Although we did not include the polarization data in the fitting procedure, our model makes reasonable theoretical predictions for the analyzing power $A_y(\theta)$ as can be seen in Figure 4. At the energies of 11.9 and 13.9 MeV the experimental results are given in reference [35] and at 14.2 MeV they are given by [36]. Since the evaluated nuclear data file did not have angular distributions data of $A_y(\theta)$ at the aforementioned elastic scattering energies, we calculated the predicted polarization asymmetry corresponding to 11.9 MeV using our fit parameter values for the elastic angular distribution obtained at 12 MeV. For the remaining 13.9 and 14.2 MeV energies, we used our parameter values obtained for the fit to the elastic angular distribution

at 14.0 MeV. We expect that our theoretical predictions for the analyzing power can be improved by including other sources of nonlocalities, such as exchange effects and coupling of the ground state elastic channel to inelastic excitations.

We have also fitted the 14 MeV angular distribution elastic scattering data using a conventional optical potential model by setting the gradient term $\rho(r)$ to zero. This energy was chosen as analyzing power data are available at 13.9 and 14.2 MeV, which provide more physical constraints on the values of the potential parameters. The corresponding fit to the elastic angular distribution is shown in Figure 5. Clearly, the overall behavior of the differential cross section is reproduced but the fine details are less well described compared to the VDOP fit at the same energy as shown in Figure 1 (b). In addition, fits to the data became harder to achieve as the incident energy increased. In particular, the large-angle backward scattering minima at 18 and 20 MeV and the details of the differential cross sections were much less well reproduced compared to the corresponding VDOP fits. Further, the theoretical prediction for the analyzing power, $A_y(\theta)$, presented in Figure 6 still needs to be improved, as was the case for the VDOP, but agreement with experimental data around 60° is clearly better for the prediction of the proposed velocity-dependent optical potential.

5 Discussion and conclusion

In a previous work Cooper and Mackintosh [11] showed that good fits to low energy scattering of either protons or neutrons from ^{12}C or ^{16}O out to 180° could not be accomplished using only local optical potentials. They introduced a nonlocality by means of parity-dependent potentials which contained factors $(-)^L$, where L is the orbital angular momentum of the projectile relative to the target nucleus. In this work we introduce a different type of nonlocality in the form of a derivative term. This nonlocality, described by a position-dependent effective mass which multiplies the first order derivative term of the scattering wave function, is presumed to be a consequence of the static interaction of the incident nucleon with the other nucleons in the nuclear medium. Its physical origin will be the object of a separate investigation [19]. One argument justifying the introduction of our velocity dependent term, is that the magnitude of the central part of the optical potential depends much less on energy than for fits using only local potentials.

Another argument is that we obtain excellent fits to the pronounced minima, especially at 18 and 20 MeV, in the angular distribution of the elastic cross section at large angles, shown in Figure 2, that can otherwise not be fitted well [11, 14]. Furthermore, our predicted analyzing powers have trends that are in agreement with experiment.

The proposed velocity-dependent potential has a total number of 12 fit parameters given in Tables 1 and 2. This is compared to conventional optical models where the typical number of fit parameters ranges between nine and twenty [33, 34]. In this work, the details of the differential cross section fits were sensitive to both the spin-orbit and velocity-dependent terms, in particular to their strengths and radii. The best fits, shown in Figures 1 and 2, were obtained with the peak of $\rho(r)$ located within the region of the diffused nuclear surface. This supports the hypothesis that $\rho(r)$ may be viewed as the gradient of the nuclear mass density [21]. By inspecting Tables 1 and 2, it is clear that the radius of the spin-orbit term decreased monotonically as the incident energy increased. In addition, the fit values for the strengths of the real and imaginary parts V_0 and W showed only a small energy dependence. The theoretical predictions of our model for the analyzing power given in Figure 4 can probably be improved by including other sources of nonlocalities such as exchange processes and channel coupling to inelastic excitations.

E_{lab} <i>MeV</i>	U_0 <i>MeV</i>	r_0 <i>fm</i>	a_0 <i>fm</i>	W <i>MeV</i>	r_w <i>fm</i>	a_w <i>fm</i>
12	44.5	1.30	0.45	6.2	1.34	0.39
14	44.7	1.31	0.46	5.7	1.30	0.45
16	40.1	1.39	0.37	6.3	1.47	0.23
18	40.1	1.31	0.56	6.6	1.32	0.40
20	39	1.35	0.51	6.5	1.36	0.47

Table 1: Velocity-dependent optical model fit parameters for the $N - {}^{12}C$ angular distribution elastic scattering. The potential terms are given by equations (6) and (7)

In summary, we have introduced into the optical model potential a nonlocality that is normally not used to describe nucleon-nucleus elastic scattering. It is in the form of a derivative term, multiplied by a function that depends on a position dependent effective mass. Our excellent fits to the elastic angu-

E_{lab} <i>MeV</i>	V_{so} <i>MeV</i>	r_{so} <i>fm</i>	a_{so} <i>fm</i>	ρ_0 –	r_ρ <i>fm</i>	a_ρ <i>fm</i>
12	$16.99 + 2.80 i$	1.15	0.08	–1.82	1.80	0.12
14	$11.59 + 3.67 i$	1.03	0.11	–1.71	1.50	0.13
16	$24.72 + 4.83 i$	1.00	0.11	–1.46	1.30	0.15
18	$23.56 + 15.45 i$	0.81	0.15	–2.27	1.33	0.15
20	$17.19 + 21.25 i$	0.80	0.19	–2.05	1.20	0.15

Table 2: Velocity-dependent optical model fit parameters for the $N -^{12}C$ angular distribution elastic scattering. The potential terms are given by equations (6) and (7)

lar distribution, especially at large angles, justify engaging in an exploration of how our nonlocality is related to the conventional nonlocalities due to exchange effects and coupling to inelastic channels, or whether our nonlocality is indeed related to a change of effective mass of the projectile in the medium of the target nucleus, and hence represents a new effect.

References

- [1] H. Feshbach, C.E. Porter and V. E. Weisskopf, *Phys. Rev.* **96**, 448 (1954).
- [2] A.K. Kerman, H. McManus and R. M. Thaler, *Ann. Phys. (N. Y.)* **8**, 551, (1955).
- [3] R. Crespo, R. C. Johnson, J. A. Tostevin, R.S. Mackintosh and S. G. Cooper, *Phys. Rev.* **49**, 1091 (1994).
- [4] E. D. Cooper, S. Hama, B. C. Clark and R. L. Mercer, *Phys. Rev. C* **47**, 297, (1993).
- [5] P. K. Deb, B. C. Clark, S. Hama, K. Amos, S. Karataglidis, and E. Cooper, *Phys. Rev.* **72**, 014608 (2005), and references therein.
- [6] B. C. Clark, S. Hama, and R. L. Mercer, in Proceedings of the Workshop on the Interaction Between Medium Energy Nucleons in Nuclei (Indiana University Cyclotron Facility, Bloomington, Indiana), AIP Conf. Proc. No. 97, edited by H. O. Meyer (AIP, New York, 1982), p. 260.
- [7] G. Rawitscher, *Phys. Rev.C* **31**, 1173 (1984).
- [8] K. Amos, L. Canton, G. Pisent, J. P. Svenne and D. van der Knijff, *Nucl. Phys. A* **728**, 65 (2003).
- [9] E. Cereda, M. Pignanelli, S. Micheletti, H. V. von Geramb, M. N. Harakeh, R. De Leo, G. D’Erasmus, and A. Pantaleo *Phys. Rev.C* **26**, 1941 (1982).
- [10] F. G. Perey and B. Buck, *Nucl. Phys. A* **32** , 353 (1962).
- [11] S. G. Cooper and R. S. Mackintosh, *Phys. Rev.C* **54**, 3133 (1996).
- [12] S. G. Cooper, *Nucl. Phys. A* **618**, 87 (1997).
- [13] G. H. Rawitscher, D. Lukaszek, R. S. Mackintosh and S. G. Cooper, *Phys. Rev.C* **49**, 1621 (1994).
- [14] G. H. Rawitscher and D. Lukaszek, *Phys. Rev.C* **69**, 044608 (2004).
- [15] A. Detluva, *Phys. Rev. C* **79**, 021602(R), (2009).

- [16] P. Ring and P. Schuck, *The Nuclear Many Problem* (Springer Verlag, New York, 1980), p. 211
- [17] O. von Roos, *Phys. Rev. B* **27**, 7547 (1981).
- [18] M. I. Jaghoub, *Eur. Phys. J. A* **28**, 253, (2006).
- [19] M. Jaghoub and G. Rawitscher, manuscript in preparation.
- [20] L. G. Arnold and B. C. Clark, *Phys. Lett. B* **84**, 46, (1979).
- [21] L.S. Kisslinger, *Phys. Rev.* **98**, 761 (1955).
- [22] M. Razavy, G. Field and J. S. Levinger, *Phys. Rev.* **125**, 269 (1962).
- [23] A. E. S. Green, D. E. Rio and T. Ueda *Phys. Rev. A* **24**, 310 (1981).
- [24] M. R. Geller, and W. Kohn, *Phys. Rev. Lett.* **70**, 3103 (1993).
- [25] L. I. Serra and E. Lipparini, *Euro. Phys. Lett.* **40**, 667 (1997).
- [26] I. Gómez, E. Domínguez-Adame, and P. Orellana, *Physica E* (Amsterdam) **18**, 372 (2003).
- [27] M. I. Jaghoub, *Eur. Phys. J. A* **27**, 99, (2006).
- [28] M. I. Jaghoub, *Phys. Rev. A* **74**, 032702, (2006).
- [29] J.M. Levy-Leblond, *Phys. Rev. A* **52**, 1845 (1995).
- [30] A. D. Alhaidari, *Phys. Rev. A* **27**, 66, 042116, (2002).
- [31] A.R. Plastino, A. Rigo, M. Casas, F. Garcias, A. Plastino, *Phys. Rev. A* **60**, 4318, (1999).
- [32] Evaluated Nuclear Data File, Library: CENDL-3.1, Sub-Library: NSUB=10 (N), Authors: J. S. Zhang, Y. L. Han, X. J. Sun, H. C. Wu, File: MF4 Angular distributions of secondary particles, Section MT2 (N,EL)L0 Elastic scattering cross section for incident particles
- [33] J. H. Dave and C. R. Gould, *Phys. Rev. C* **28**, 2212 (1983).
- [34] A.J. Koning and J.P. Delaroche, *Nucl. Phys. A* **713** 231 (2003).

- [35] E. Woye, W. Tornow, G. Mack, C. E. Floyd, P. P. Guss, K. Murphy, R. C. Byrd, S. A. Wender, R. L. Walter, T. B. Clegg and W. Wylie, *Nucl. Phys. A* **394**, 139, (1983).
- [36] R. Casparis, B. Th. Leemann, M. Preiswerk, H. Rudin, R. Wagner, P. Zupranski, *Nucl. Phys. A* **263**, 285, (1976).

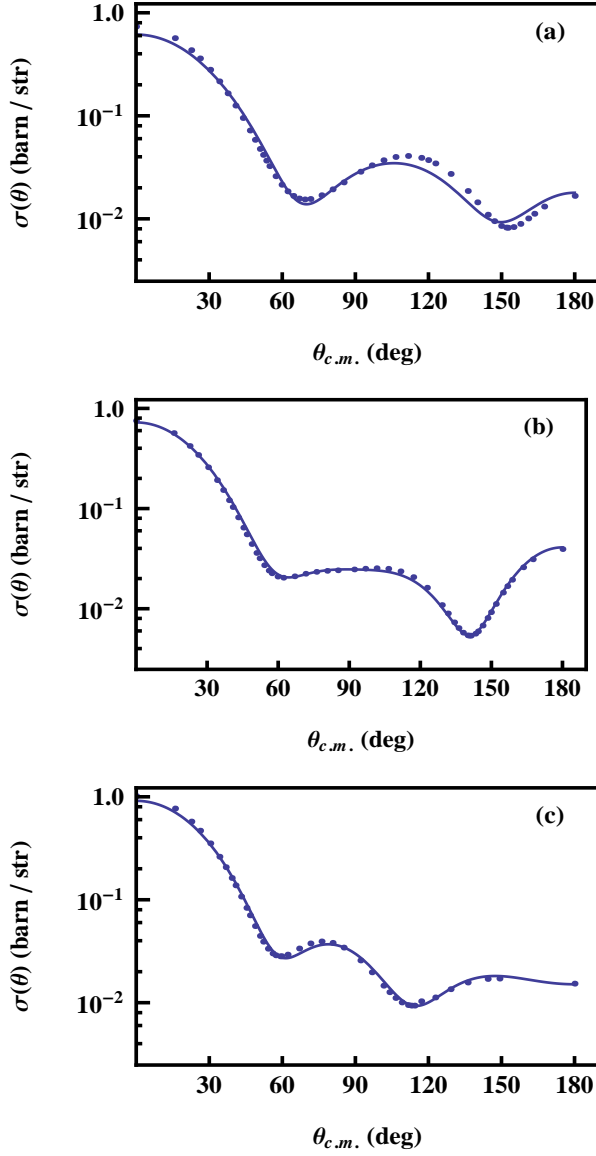


Figure 1: The velocity-dependent optical potential fits for $N - {}^{12}\text{C}$ elastic scattering at 12 (a), 14 (b) and 16 (c) all in units of MeV. The model parameters are given in Tables 1 and 2. The data is obtained from reference [32].

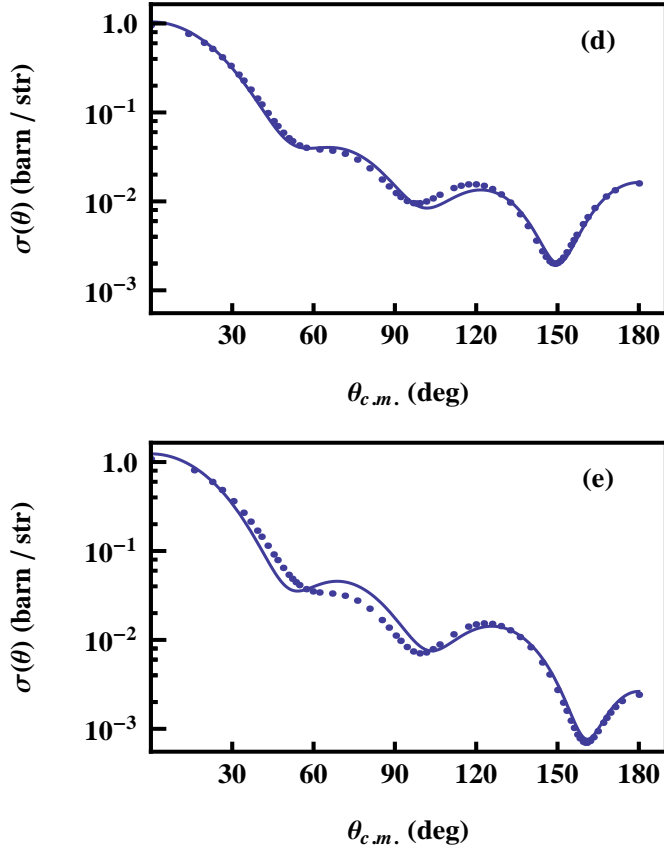


Figure 2: The velocity-dependent optical potential fits for $N -^{12}C$ elastic scattering at 18 (d) and 20 (e) in units of MeV. The pronounced minima at large backward scattering angles are evident. The model parameters are given in Tables 1 and 2. The data is obtained from reference [32].

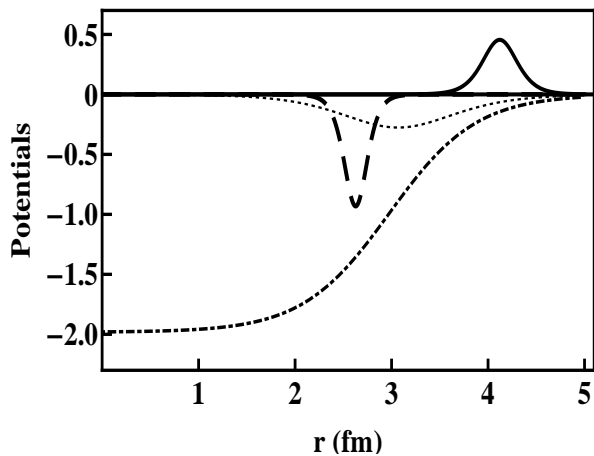


Figure 3: The potential parts of the proposed velocity-dependent optical model at a neutron incident energy of 12 MeV. Central real part (dash - dotted), central imaginary part (dotted), real part of the spin-orbit term (dashed) and, $\rho(r)$, the velocity-dependent term (solid).

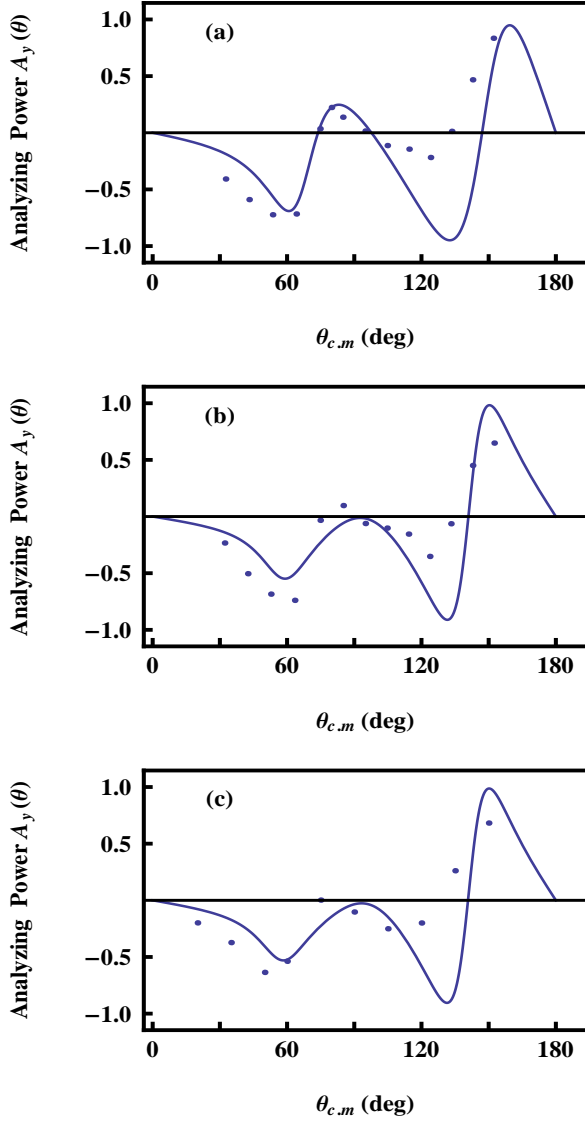


Figure 4: The velocity-dependent optical potential predictions for the analyzing power at different incident neutron energies. The experimental data for 11.9 (a) and 13.9 (b) MeV energies are taken from Ref. [35] while for the 14.2 MeV (c) the data is taken from Ref. [36].

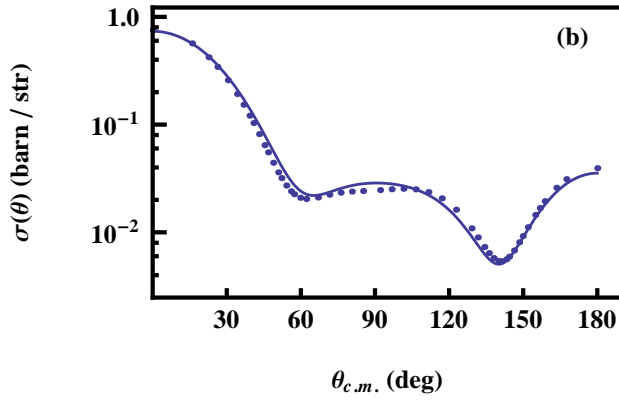


Figure 5: The conventional optical model ($\rho(r) = 0$) fit to the data at 14 MeV incident neutron energy.

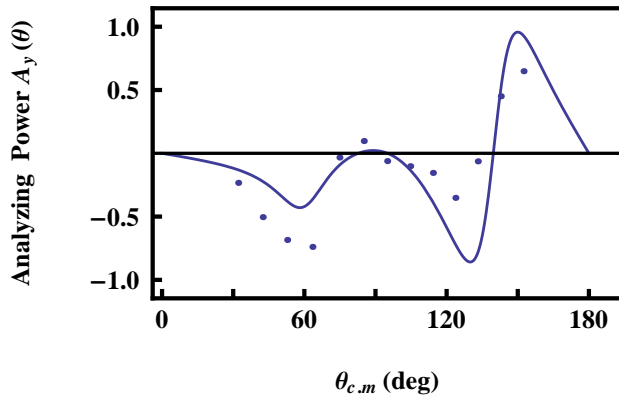


Figure 6: The conventional optical model ($\rho(r) = 0$) prediction for the analyzing power at 13.9 MeV.